J Solid State Electrochem (2010) 14:1877–1883
DOI 10.1007/s10008-010-1030-z

ORIGINAL PAPER

Electrochemical generation of ozone at PbO_2-loaded platinum screens

Mohamed I. Awad · Mahmoud M. Saleh

Received: 18 November 2009 / Revised: 17 January 2010 / Accepted: 8 February 2010 / Published online: 2 March 2010

Abstract Ozone (O_3) has been electrochemically generated on PbO_2-loaded Pt screens (PbO_2/Pts) at 25 °C from H_2SO_4 solutions. The PbO_2/Pts electrodes were electrochemically and morphologically characterized by cyclic voltammetry and scanning electron microscopy (SEM), respectively. Different loadings of PbO_2 and different acid concentrations (C_{acid}) were used in this study. Higher efficiency (8%) for O_3 electrogeneration was obtained at an applied potential of 1.8 V, higher C_{acid}, and loading density of $PbO_2 \geq 9.3$ μmol cm^{-2} (of Pt screen) at room temperature. The stability of the prepared electrode was examined under the present experimental conditions. SEM images and current transients showed reasonable electrochemical and mechanical stability of the PbO_2/Pts. The data were discussed in the light of results obtained on planar Pt electrode at similar conditions.

Keywords Ozone · Oxygen · Electrolysis · Pt screen · Pb

Introduction

Ozone (O_3) is an important oxidant and is considered the first choice for better oxidation performance both from environmental and technological point of view [1, 2]. It is the first choice as disinfectant when a high purification standard of drinking water is needed [3–7]. O_3 generation via electrochemical routes has gained much attention during the last decade [8, 9]. Different anodes have been used for such applications [10–12]. Specific properties of these anodes should be guaranteed before its possible use. Among these properties, high overpotential of oxygen evolution (η_{O_2}) and high stability at high positive potentials are essential [13–15]. Dimensionally stable anodes such as Ta_2O_5 showed good performance for O_3 generation, and many reports have been released on this issue [16, 17]. On the other hand, the costly platinum electrodes suffer from the lower coulombic efficiency. Lead dioxide has been used for the production of O_3, and good results have been achieved compared to Pt [18]. As a basic requirement for high rates of the electrochemical reaction, a high-surface area and a low volume to surface ratio are crucial. The use of high-surface area electrodes such as porous electrodes for higher rates of the electrochemical reaction are well documented for many applications [19, 20]. Porous electrodes under the conditions of electrolyte flow have been used for generation of ozone. However, low efficiency and questionable stability were serious problems in such systems [21, 22].

In this present study, a porous electrode (PbO_2-loaded Pt screens (PbO_2/Pts)) is examined for ozone electrogeneration (OE) under different conditions of PbO_2 loading and the pH of the electrolyte solution. The above electrode can be a candidate for packing three-dimensional electrodes for in situ OE.

Experimental

The chemicals were of analytical grade. Deionized water was used to prepare all solutions. The Pt screen had a mesh size of 80 PPI (pore per inch) and specific surface area of ~36 cm^2/g. The mean pore opening was 0.017 cm, and the thread (wire) thickness was 0.08 cm. The Pt working electrodes were either planar Pt (1.6 mm diameter) or Pt screens (square 1.2 cm width). The counter and the

M. I. Awad (✉) · M. M. Saleh
Chemistry Department, Faculty of Science, Cairo University, Cairo, Egypt
e-mail: mawad70@yahoo.com

reference electrodes were, respectively, a spiral Pt wire and Ag/AgCl/KCl (Sat.). The planar Pt electrode was polished first with no. 2000 emery paper, then with aqueous slurries of successively finer alumina powder (particle size down to 0.06 mm) with the help of a polishing microcloth. Then, it was electrochemically pretreated in N_2-saturated 0.1 M H_2SO_4 solution by repeating the potential scan in the range of −0.2 to 1.5 V until the cyclic voltammogram (CV) characteristic for a clean Pt electrode was obtained.

The electroplating bath of PbO_2 was 0.1 M $Pb(NO_3)_2$+ 0.1 M HNO_3. The electrodeposition of PbO_2 onto the Pt screens was carried out potentiostatically at E=+1.7 V in a conventional three-electrode cell in a stirred solution purged with Ar gas. Prior to the electrodeposition of the lead dioxide, the Pt screen substrate was electrochemically pretreated similarly to the planar Pt electrode as stated above. Current densities are given on the basis of the geometrical cross-sectional area of the electrode. A potentiostat (EG&G model 273A) was used in all the measurements.

Ozone was generated potentiostatically from H_2SO_4 solutions at room temperature (25 °C). The O_3 concentration was determined by a potentiometric method that has been reported elsewhere [23, 24]. A given volume of an electrolyzed solution was injected to the iodide/iodine (I^-/I_2) redox buffer solution with a known concentration of both constituents, and the O_3 concentration was determined from the change in the open circuit potential. The scanning electron microscopy (SEM) images of the electrode surface were observed using a scanning electron microscope (KEYENCE COMPANY, Japan) at an acceleration voltage of 1.5 kV and a working distance of 7.5 mm.

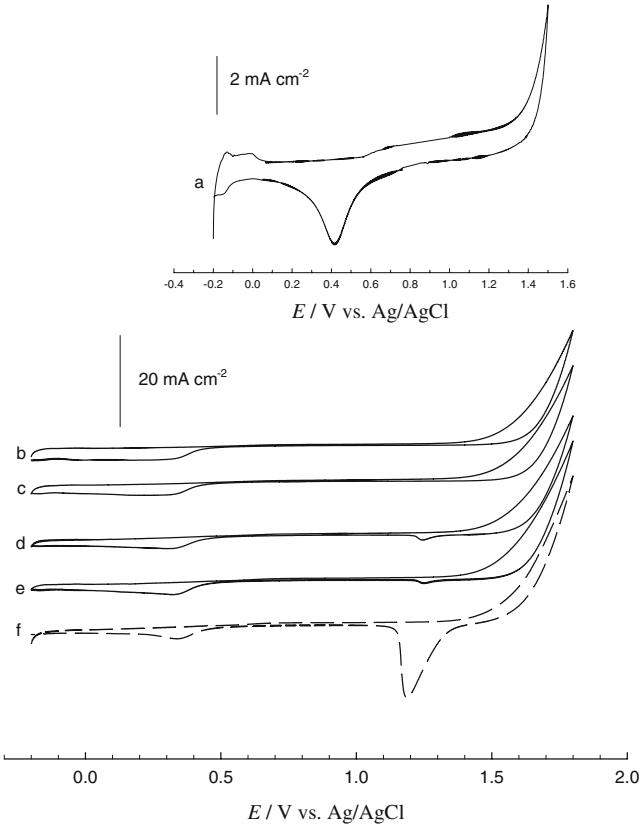

Fig. 1 Cyclic voltammograms obtained at (*a*, *b*) the bare planar Pt (1.6 mm diameter) and PbO_2/Ptp (*c*–*f*) electrodes in 0.5 M H_2SO_4. Potential scan rate, 100 mV s^{-1}. PbO_2 was electrodeposited onto the planar Pt electrode from a solution containing $Pb(NO_3)_2$ by applying a constant potential of 1.7 V for (*c*) 10, (*d*) 30, (*e*) 90, and (*f*) 300 s. The geometric surface area of all substrates is 0.02 cm^2

Results and discussion

Results on planar electrode

The OE indirectly depends on the oxygen overpotential (η_{O_2}) [17, 25]. In this section, the effects of lead dioxide loading (m_{dep}) and the pH of the electrolyte solution on the oxygen evolution are studied at PbO_2-modified planar platinum electrode (PbO_2/Ptp). Figure 1 shows the CV response of (a, b) bare Pt electrode and (c–f) PbO_2/Ptp electrodes of different extents of m_{dep} in 0.5 M H_2SO_4 at a scan rate of 0.1 V/s. The different m_{dep} were achieved by controlling the time of deposition (t_{dep}) of PbO_2 on the planar Pt electrode. The t_{dep} were (c) 10, (d) 30, (e) 90, and (f) 300 s. The voltammetric response changes dramatically with the extent of m_{dep}. Inspection of this figure reveals several interesting points:

1. The characteristic voltammetric response of the bare planar Pt is clearly shown in curve (a), i.e., the two characteristic peaks corresponding to Pt/Pt-oxide couple, and the hydrogen adsorption/desorption pattern are revealed.
2. In curves (c–f), the potential was scanned in a wide potential range to cover the potential (ca. >1.5 V), at which, the electrodeposited lead is expected to be oxidized. Curve (b) shows the voltammogram of the bare Pt electrode in the same potential range for comparison. The CV in Fig. 1 curve (c) (t_{dep}=10 s) does not show any peak at E≈1.2 V, at which, the PbO_2 is expected to be reduced [25, 26]. This means that the deposited PbO_2 cannot be detected by the cyclic voltammetric technique in this case, probably due to the low sensitivity of this technique.
3. It is noteworthy to mention that while the reduction peak of platinum-oxide (PtO_x; at ca. 0.4 V) is sharp in curve (a), broad peaks were obtained in curves (b–f). The broadening of the PtO_x reduction peak may be attributed to the higher amount of PtO_x formed at potential range up to 1.8 V. Hence, higher amount of charge is needed to reduce the thicker film. The area under the broad reduction peak (starting from ca. 0.4 V)

decreases gradually with the increase in the PbO_2 loading. In curve (f), a more sharp peak is obtained indicating lower exposed area of the underlying Pt surface, which means low amount of reduction charge.

4. In curves (d–f) upon increasing t_{dep}, a new peak emerges at around 1.2 V. The intensity of this peaks increases with the m_{dep}. This peak may be assigned to the electrochemical surface reaction represented by Eq. 1, i.e., the reduction of the lead dioxide formed upon the anodic scanning of the potential positive to 1.5 V in agreement with reported values [25, 26]:

$$PbO_2 + 3H^+ + HSO_4^- + 2e^- \rightarrow PbSO_4 + 2H_2O \quad (1)$$

It is noteworthy to mention that the anodic peak, which corresponds to the formation of lead dioxide, is not evident in the present case because it is obscured by the oxygen evolution current.

5. The reduction peaks in curves (c–f) at ca. 1.2 V are of different intensities pointing to the different m_{dep}. Interestingly, the increase in the intensity of this peak is accompanied by a concurrent decrease in the reduction peak at 0.4 V, i.e., the exposed underlying platinum area decreases. This again confirms the increase of the coverage of PbO_2 upon increasing t_{dep}.
6. The appearance of the reduction peak at around 0.4 V (corresponds to PtO_x reduction) along with that at 1.2 V (corresponds to PbO_2 reduction) in curves (d–f) indicates that the voltammetric behavior is a combination of the underlying platinum substrate and the electrodeposited lead dioxide. This points to the incomplete covering of the underlying substrate with the loaded PbO_2. Thus, both electrochemical measurements and SEM (Fig. 3) consistently confirm the existence of pinholes within the loaded PbO_2 through which the electrolyte can access the substrate.

Figure 2 shows the anodic polarization curves obtained at the (a) bare Pt and (b–d) PbO_2/Ptp electrodes, with different m_{dep} in 0.5 M H_2SO_4 solutions at a scan rate of 10 mV s^{-1} and 25 °C. The onset potential of the oxygen evolution is shifted anodically upon loading PbO_2. At the same potential, the current density sustained by PbO_2/Ptp electrodes is shifted to lower current densities compared with that sustained by the bare Pt. This means that the modification of the Pt electrode by PbO_2 inhibited the oxygen evolution. This anodic potential shift is of primary importance for an electrode to be suitable for OE. The inhibition of the oxygen evolution can be achieved in several ways including, for example, the selection of a suitable electrode with naturally high η_{O_2} electrolyte with low pH and selection of a suitable electrolyte, for example, fluoride-containing electrolytes [27]. In this direction, the effect of C_{acid} was studied (data

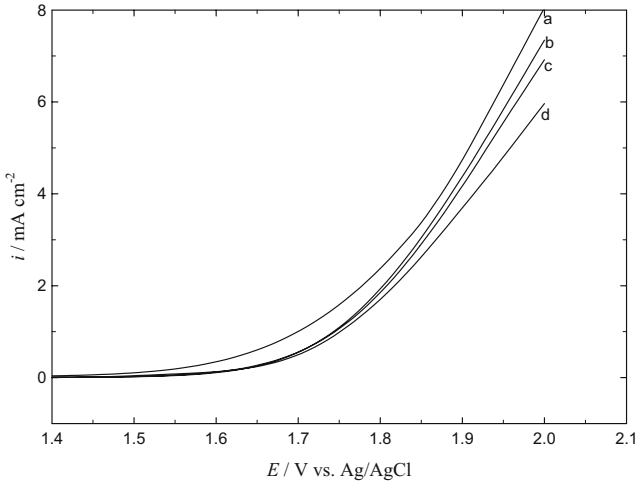

Fig. 2 Anodic polarization curves obtained at (*a*) the bare Pt (1.6 mm diameter) and PbO_2/Ptp (*b–d*) electrodes in 0.5 M H_2SO_4. Potential scan rate, 10 mV s^{-1}. PbO_2 was electrodeposited onto the planar Pt electrode from a solution containing $Pb(NO_3)_2$ by applying a constant potential of 1.7 V for (*b*) 30, (*c*) 90, and (*d*) 300 s. The geometric surface area of all substrates is 0.02 cm^2

are not shown), and as expected, an increase in C_{acid} cathodically shifted the onset potential of the oxygen evolution. Higher concentration of the acid may have an adverse effect, which is the simultaneous electrogeneration of persulfate and ozone [28].

Ozone electrogeneration on PbO_2-loaded Pt screen

Effect of PbO_2 loading

Figure 3 shows the SEM images taken for the unmodified (image a) and PbO_2-modified (image b) Pt screen samples (PbO_2/Pts). The PbO_2 is deposited in a granular shape (of size ca. 25 nm) forming an agglomerate structure (image b). It is revealed that the underlying Pt screen is incompletely covered with lead dioxide in consistent with the results obtained from the electrochemical characterization shown above in Fig. 1.

The nature of the electrode as well as the electrolyte concentration in addition to the applied potential used for electrolysis are among the most important factors affecting the efficiency of OE. Low temperature also plays a vital role in OE because the half-life time of O_3 aqueous solution is relatively short at room temperature (ca. 15 and 8 min at 25 °C and 35 °C, respectively) [29]. The OE is studied at the bare and PbO_2-modified Pt screens under different conditions of PbO_2 loading (m_{dep}), applied potential for electrolysis, and C_{acid}. The coulombic efficiency (*CE*) of the OE was determined from the following equation:

$$CE = \frac{n_{Exp}}{n_{th}} \times 100 = \frac{6Fn_{Exp}}{Q_{th}} \times 100 \quad (2)$$

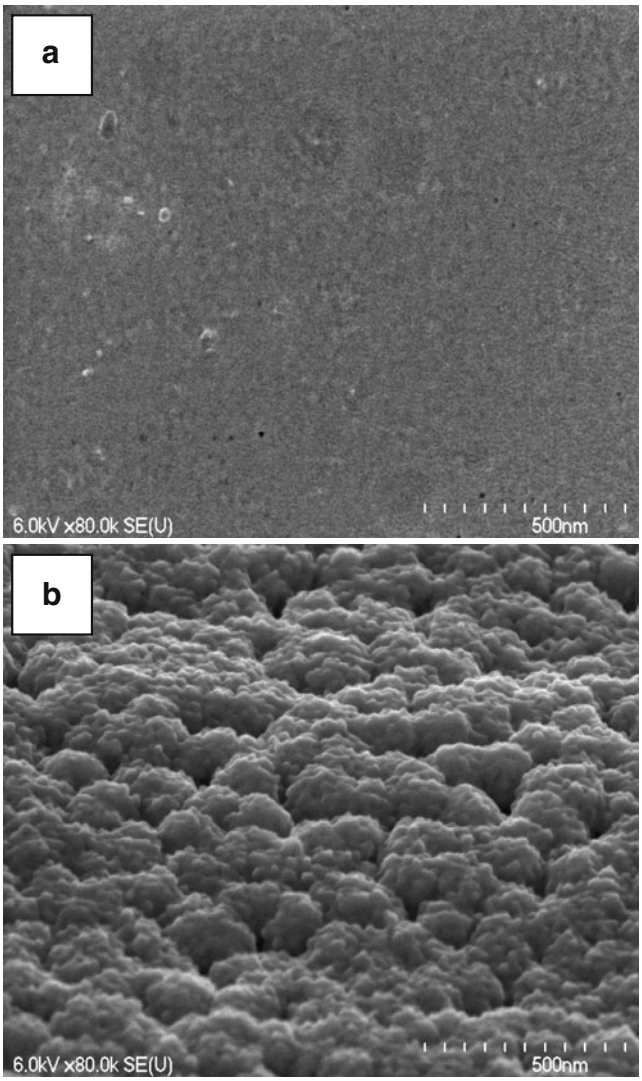

Fig. 3 Scanning electron micrographs obtained for (**a**) the bare Pt screen and (**b**) PbO_2/Pts electrodes. PbO_2/Pts electrode was prepared by electrodeposition of PbO_2 from 0.1 M $Pb(NO_3)_2$ dissolved in 0.5 M HNO_3 by applying constant potential of 1.7 V for 5 min

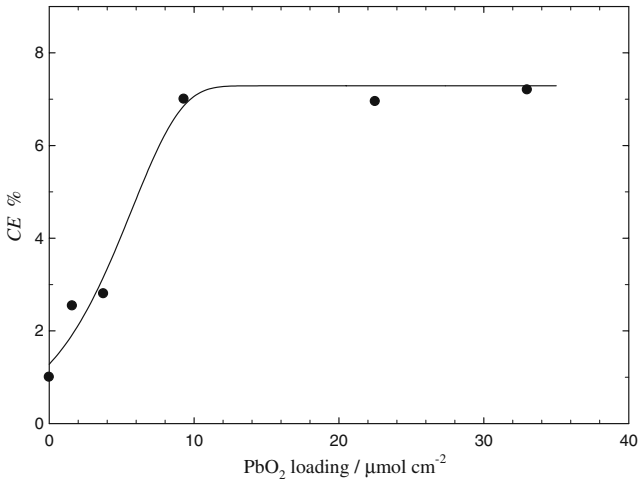

Fig. 4 Effect of PbO_2 loading on O_3 electrogeneration efficiency. O_3 was generated from 0.5 M H_2SO_4 by applying a constant potential of 1.8 V vs. Ag/AgCl

where n_{Exp} and n_{th} (Q_{th}/zF) are the number of moles of O_3 obtained experimentally and calculated theoretically, respectively, z is the number of electrons (equals six in the present case), and Q_{th} equals it (where i is the current applied for a time period t). Figure 4 and Table 1 show the effect of m_{dep} on the CE and C_{O_3} of the OE, respectively. The m_{dep} (achieved by applying a constant potential (1.7 V) for different time periods) were found to be 1.60, 3.75, 9.30, and 33.0 μmol cm^{-2} (of Pt screen; assuming 100% of current efficiency of PbO_2 formation). These loadings correspond to t_{dep} of 10, 30, 90, and 300 s, respectively. A significant increase in the efficiency of OE with the increase of m_{dep} is revealed. The bare Pt screen shows a poor efficiency of the OE of around 1% in agreement with the literature [30, 31]. In the present work, PbO_2/Pts electrode shows double of this amount on loading 1.60 μmol cm^{-2} of PbO_2. The efficieny increases with the increase in the m_{dep} until it reaches constant higher values at $m_{dep} \geq 9.30$ μmol cm^{-2}. It is noteworthy to mention that, to the best of our knowledge, the highest reported values of OE efficiency at lead dioxide electrodes is around 13% [32]. However, this value was obtained in the presence of very high C_{acid} (50% H_3PO_4) and at relatively low temperature (8.5 °C). On the other hand, at 20 °C, the CE of OE using relatively high current density (0.8 A cm^{-2}) from 3 M H_2SO_4 containing F^- ions has been reported to be 6% [27]. The CE obtained here under mild conditions (25 °C and 0.5 M H_2SO_4) and by applying a constant potential of 1.8 V (corresponds to around 50 mA cm^{-2}) may be considered to be a superior value. The increase in the OE efficiency with the increase in the PbO_2 loading can be attributed to the anodic shift of the oxygen evolution upon loading PbO_2 (see Fig. 2). This

Table 1 C_{O_3} obtained at the bare Pt screen (zero loading) and PbO_2/Pts electrodes of different loading

Loading time/s	PbO_2 loading[a]/μmol cm^{-2}	$[O_3]$/μM
0	0.0	0.5
10	1.60	2.4
30	3.75	2.4
90	9.30	4.1
300	33.0	4.6

The ozone was generated potentiostatically at 1.8 V in 0.5 M H_2SO_4

[a] The PbO_2 loading was estimated from the amount of the charge consumed during its electrodeposition at 1.7 V from the electroplating bath by assuming consumption of two electrons for the electrodeposition

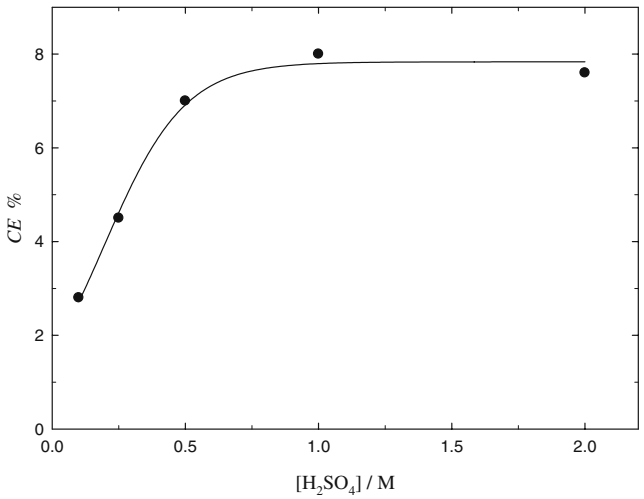

Fig. 5 Effect of C_{acid} on O_3 electrogeneration efficiency. O_3 was generated from H_2SO_4 by applying a constant potential of 1.8 V vs. Ag/AgCl. m_{dep}=33.0 μmol cm^{-2}

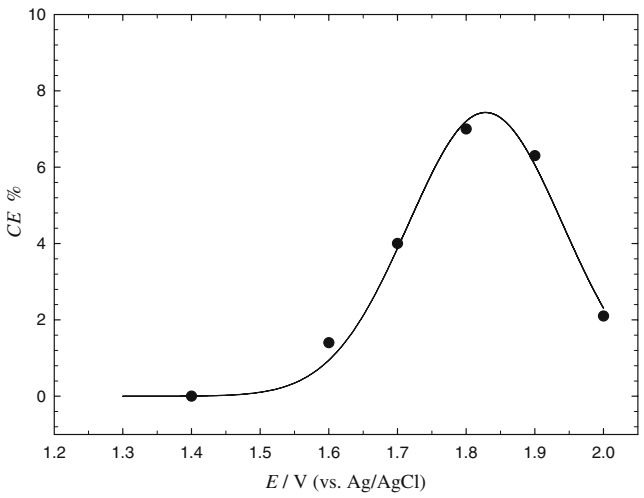

Fig. 6 Effect of applied potential on O_3 electrogeneration efficiency. C_{acid}=0.5 M and m_{dep}=33.0 μmol cm^{-2}

anodic shift may give a chance for O_3 evolution at the expense of the oxygen evolution, which is thermodynamically favorable over the former one (see Eqs. 3 and 4). Another possible reason could be the change in the interficial properties in such a way that facilitates the conversion of the adsorbed oxygen ($(O_2)_{ads}^{*}$) to O_3 (Eq. 5). This occurs via an optimum residence time of adsorbed oxygen atom $(O^{\cdot})_{ads}^{*}$ on the PbO_2 surface for further reaction with generated O_2, i.e., the probability of the assembly of three oxygen atoms increases [33, 34].

$$O_3 + 6H^+ + 6e = 3H_2O \quad E^o = 1.51\,V \tag{3}$$

$$O_2 + 4H^+ + 4e = 2H_2O \quad E^o = 1.23\,V \tag{4}$$

$$(O_2)_{ads}^{*} + (O^{\cdot})_{ads}^{*} \rightarrow O_3 \uparrow \tag{5}$$

where "*" refers to the surface coverage by the oxygenated species participating in the OE. The optimum m_{dep} that achieved the highest possible efficiency equals 33 μmol cm^{-2} (of Pt screen). Thus, this loading will be considered as the optimum one and will be used hereafter in studying the effect of other factors on the O_3 electrogeneration efficiency.

Table 2 C_{O_3} obtained at PbO_2/Pts electrode in the presence of different C_{acid}

$[H_2SO_4]$/M	0.10	0.25	0.50	1.0
$[O_3]$/μM	0.50	2.0	5.0	6.0

The PbO_2 loading, 33.0 μmol cm^{-2}. The ozone was generated potentiostatically at 1.8 V

Effect of the acid concentration

Figure 5 and Table 2 show the effect of acid concentration (C_{acid}) on the *CE* and C_{O_3}, respectively. Ozone was electrogenerated potentiostatically at 1.8 V and m_{dep}= 33 μmol cm^{-2}. The efficiency increases with the increase in the C_{acid}. This can be attributed to the excessive incease in the number of moles of O_3. The coulombs passed, however, do not increase as fast as the C_{O_3} due to the shift in the anodic potential (see Eq. 2). The current efficiency slightly decreases in 2 M H_2SO_4 compared with that in 1 M H_2SO_4. This could be attributed to the possible electrogeneration of persulfate along with ozone in high acid concentration. It has been reported that the persulfate electrogeneration in H_2SO_4 concentration higher than 0.5 is significant [35]. The *CE* does not significantly increase at $C_{acid} \geq 0.5$ M. The independence of the observed *CE* on the C_{acid} when it is higher than 0.25 M may indicate that the reaction is zero order with respect to C_{acid} in this range of concentration. However, this reaction order is determined at constant overpotential not at constant potential. The order determined at constant potential is of chemical significance as has been reported [36]. The two reaction orders are interrelated by the following equation:

$$v(\eta) = v(E) - \gamma \tag{6}$$

where $v(\eta)$ and $v(E)$ are the reaction orders at constant overpotential and constant potential, respectively, and γ is

Table 3 C_{O_3} obtained at PbO_2/Pts electrode at different potentials in 0.5 M H_2SO_4

Potential/V	1.7	1.8	1.9	2.0
$[O_3]$/μM	0.8	5.0	6.5	3.2

The PbO_2 loading, 33.0 μmol cm^{-2}

the transfer coefficient. The Tafel slope of the oxygen evolution, b, was calculated from the semilogarithmic plot of the current versus potential (data are not shown) and was found to be around 120 mV/decade. The Tafel slope can probe the rate determining step (rds) of the oxygen evolution. Tafel slope of 120 mV/decade suggests that the water discharge is the rds (Eq. 7), and a slope of 40 mV/decade suggests that Eq. 8 is the rds [37]. In the present case, the Tafel slope of 120 mV/decade suggests that the water discharge is the rds.

$$S + H_2O \rightarrow S - OH + H^+ + e \quad (7)$$

$$S - OH \rightarrow S - O + H^+ + e \quad (8)$$

where S denotes a surface active site.

The transfer coefficient (γ) was then estimated from the Tafel slope, b, i.e., from $b=2.303RT/\gamma F$, and it is found to be 0.5. Substituting this value in Eq. 6 and considereing the reaction order at constant overpotential equals zero as pointed above gives a fractional reaction order of 0.5. The fractional reaction order is oftenly observed for oxygen evolution at oxide electrodes and was explained in terms of acid–base equilibria at the oxide surface [28, 38].

In the present study, the C_{acid} of 0.5 M could be selected as the optimum one for three reasons: the first is that at high C_{acid}, there is a high probability of electrogeneration of persulphate concurrently with O_3 [35]. The second, OE in the presence of low C_{acid} is another advantage because, in this case, O_3 can be used in on-site applications. The third, OE requires a high applied anodic potential. Thus, using low pH will decrease the half-life time of the electrode, which is essential for industrial applications. In the presence of high acid concentration, the deposited lead dioxide may be partially dissolved according to the reaction shown in Eq. 1 [39].

Effect of applied potential

The optimization of the effect of the applied potential (E) on the OE efficiency was carried out at the optimum concentration of H_2SO_4 (0.5 M) and PbO_2 loading (9.3 μmol cm^{-2} (of Pt screen)), and the results are shown in Fig. 6 and Table 3. The E values were selected over a suitable range that started from a value little lower than the thermodynamic potential of O_2 evolution and extended over a wide range. As shown in Fig. 6, the dependence of CE on the applied potential is of parabolic behavior. The current efficiency at $E<1.51$ (thermodynamic value for the O_3 evolution) is nill. Current efficiency increases up to E around ~1.8 V before it decreases to lower values. A possible reason for this decrease could be the concurrent electrogeneration of persulphate (according to Eqs. 9 and 10 with standard potentials of 1.77 and 1.88 V (SCE), respectively [32]) along with O_3:

$$2SO_4^{2-} \rightarrow S_2O_8^{2-} + 2e^- \quad (9)$$

$$2HSO_4^- \rightarrow S_2O_8^{2-} + 2H^+ + 2e^- \quad (10)$$

In addition to this reason, applying a higher E may produce local heating in the vicinity of the electrode. This may lead to the decomposition of O_3, which is characterized by a very short half-life time at high temperature [27, 29].

Stability of PbO_2/Pts electrode

The stability of the PbO_2/Pts electrode with loading extent of 33 μmol cm^{-2} was examined by taking SEM (Fig. 7) before (Fig. 3b) and after (Fig. 7) being used for OE for 5 h. This time of operation may be short but could be quite enough for the purpose of this study. By comparing the two images, one can notice that there is an apparent partial removal of PbO_2 from the platinum screen. However, when this electrode was reused for electrolysis, it was found that the current efficiency was not significantly changed. This could be understood in view of the results shown in Fig. 4 in which a constant CE was obtained at loading extent ≥9.3 μmol cm^{-2}. Increasing the stability of the PbO_2 deposits is now under investigation. It can be improved by, for example, using a suitable bath for electrodeposition or controlling the structure of the deposited PbO_2.

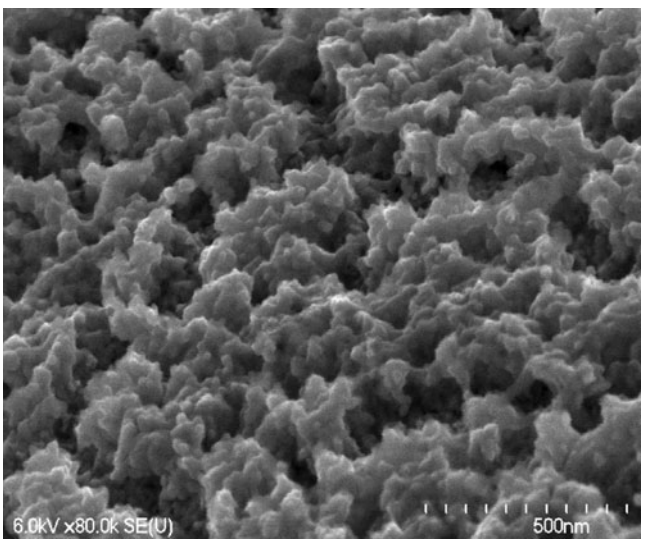

Fig. 7 Scanning electron micrograph obtained for PbO_2/Pts electrode (after being used for electrolysis for 5 h at constant potential (1.8 V) in 0.5 M H_2SO_4). m_{dep}=33.0 μmol cm^{-2}

Summary and conclusions

Ozone was electrogenerated from H_2SO_4 solutions on PbO_2/Pts electrodes at different operating conditions. The electrode was characterized by SEM and CV. Higher efficiency of O_3 generation was obtained at 1.8 V in 0.5 M H_2SO_4 at a loading density of 33 μmol cm^{-2}. The behavior of PbO_2/Pts electrodes was discussed in the light of the results obtained at planar PbO_2/Ptp electrode. The results obtained were compared with respect to the literature. Further work should be done for better stability and also using this porous material for a flow-through reactor.

References

1. Jozwiak WK, Mitros M, Kałuzna-Czaplińska J, Tosik R (2007) Dyes Pigm 74:9
2. Serdar O, Bulent Z, Kiroglu ZF (2006) J Food Eng 75:396
3. Von Gunten U (2003) Wat Res 37:1469
4. Leshem EN, Pines DS, Ergas EG, Reckhow DA (2006) J Environm Eng 132:324
5. Zhao W, Wu Z, Wang D (2006) J Hazard Mater B137:1859
6. Yasuda M (2005) Electrochem Solid State Lett 8:J13
7. Oztekin S, Zorlugenc B, Zorlugenc FK (2006) J Food Eng 75:396
8. Kishimoto N, Morita Y, Tsuno H, Oomura T, Mizutani H (2005) Wat Res 39:4661
9. Meng MX, Hsieth JJ (2000) Tappi J 83:67
10. Foller PC, Kelsall GH (1993) J Appl Electrochem 23:996
11. Da Silva LM, Franco DV, Forti JC, Jardim WF, Boodts JFC (2006) J Appl Electrochem 36:523
12. Amadelli R, Armelao L, Velichenko A, Nikolenko NV, Girenko DV, Kovalyov SV, Danilov FI (1999) Electrochim Acta 45:713
13. Ye Z, Meng H, Chen D, Yu H, Huan Z (2008) Solid State Sci 10:346
14. Rashkova V, Kitova S, Vitanov T (2007) Electrochim Acta 52:3794
15. Li WS, Chen HY, Long XM, Wu FH, Wu YM, Yan JH, Zhang CR (2006) J Power Sources 158:902
16. Da Silva LM, De Faria LA, Boodts JFC (2003) Electrochim Acta 48:699
17. Santana MHP, De Faria LA, Boodts JFC (2004) Electrochim Acta 49:1925
18. Katsuki N, Takahashi E, Toyoda M, Kurosu T, Lida M (1998) J Electrochem Soc 145:2358
19. Saleh MM (2007) J Solid State Electrochem 11:811
20. Saleh MM, Awad MI, Okajima T, Suga K, Ohsaka T (2007) Electrochim Acta 52:3095
21. Awad MI, Saleh MM, Ohsaka T (2006) J Electrochem Soc 153: D207
22. Kim K, Korshin GV (2008) Ozone Sci and Eng 30:113
23. Awad MI, Ohsaka T (2004) Electrochem Comm 6:1135
24. Awad MI, Oritani T, Ohsaka T (2003) Anal Chem 75:2688
25. Czerwinski A, Zelazowska M (1997) J Power Sources 64:29
26. Czerwinski A, Zelazowska M, Grdeń M, Kuc K, Milewski JD, Nowacki A, Wojcik G, Kopczyk M (2000) J Power Sources 85:49
27. Babak AA, Amadelli R, Fateev VN (1998) Russ J Electrochem 34:149
28. Krishtalik LI (1981) Electrochim Acta 26:329
29. Beaufils Y, Bowen P, Wenzel C, Comninellis Ch (1998) Proc Electrochem Soc 97(28):171
30. Awad MI, Sata S, Kaneda K, Ikematsu M, Okajima T, Ohsaka T (2006) Electrochem Comm 8:1263
31. Seader JD, Tobias CW (1952) Ind Eng Chem 44:2207
32. Feng J, Johnson DC, Lowery SN, Carey J (1994) J Electrochem Soc 141:2708
33. Foller PC, Tobias CW (1981) J Phys Chem 85:3238
34. Foller PC, Tobias CW (1982) J Electrochem Soc 129:506
35. Scheler I, Wabner D (1990) Naturforsch Z 45b:892
36. Da Silva LM, De Faria LA, Boodts JFC (2001) Electrochim Acta 46:1239
37. Da Silva LM, Boodts JFC, De Faria LA (2001) Electrochim Acta 46:1369
38. Angelinetta C, Falciola M, Trasatti S (1986) J Electroanal Chem 205:347
39. Monahov B, Pavlov D (1993) J Appl Electrochem 23:1244